for the 12 runs on the g.s.-4.4-MeV separation is then 1.5 keV and for the 8 runs on the g.s.-7.6-MeV separation is 2.5 keV.

In conclusion, the result of the present measurement of the excitation energy of the second excited state of ^{12}C is in excellent agreement with two other recent measurements where other techniques have been employed. The excitation energy so determined reduces the theoretical reaction rate of stellar helium burning by a factor of ≈ 3. The energy of the first excited state of ^{12}C as determined by the present charged-particle technique differs from the best γ-ray measurements by slightly more than the combined uncertainties.

†Work supported by the National Science Foundation under Grant No. Gp-15560.

[1]W. A. Fowler, G. R. Caughlan, and B. A. Zimmerman, Ann. Rev. Astronomy Astrophys. 5, 525 (1967).
[2]E. M. Burbidge, G. R. Burbidge, W. A. Fowler, and F. Hoyle, Rev. Mod. Phys. 29, 547 (1957).
[3]J. H. E. Mattauch, W. Thiele, and A. H. Wapstra, Nucl. Phys. 67, 1 (1965).
[4]C. W. Cook, W. A. Fowler, C. C. Lauritsen, and T. Lauritsen, Phys. Rev. 107, 508 (1957).
[5]J. Benn, E. B. Dally, H. H. Muller, R. E. Pixley, H. H. Staub, and H. Winkler, Phys. Letters 20, 43 (1966).
[6]C. P. Browne, W. E. Dorenbusch, and J. R. Erskine, Phys. Rev. 125, 992 (1962).
[7]F. Ajzenberg-Selove and T. Lauritsen, Nucl. Phys. A114, 1 (1968).
[8]S. M. Austin, G. F. Trentelman, and E. Kashy, Bull. Am. Phys. Soc. 15, 1662 (1970).
[9]S. J. McCaslin, F. M. Mann, and R. W. Kavanagh, Bull. Am. Phys. Soc. 15, 1598 (1970).
[10]H. Stocker, A. A. Rollefson, A. F. Hrejsa, and C. P. Browne, Phys. Rev. C 4, 930 (1971).
[11]F. H. O'Donnell, Ph.D. dissertation, University of Notre Dame, 1966 (unpublished).
[12]E. R. Cohen and J. W. M. DuMond, Rev. Mod. Phys. 37, 537 (1965).
[13]C. Chasman, K. W. Jones, R. A. Ristinen, and D. E. Alburger, Phys. Rev. 159, 830 (1967).
[14]J. J. Kolata, R. Auble, and A. Galonsky, Phys. Rev. 162, 957 (1967).
[15]C. Chasman and R. A. Ristinen, Phys. Rev. 159, 915 (1967).
[16]F. H. O'Donnell and C. P. Browne, Phys. Rev. 158, 957 (1967).

PHYSICAL REVIEW C VOLUME 4, NUMBER 4 OCTOBER 1971

Real and Virtual Radiation in Electron-Nucleus Scattering*

W. W. Gargaro† and D. S. Onley
Ohio University, Athens, Ohio 45701
(Received 25 March 1971)

Expressions are developed for the virtual photon spectrum and for the bremsstrahlung cross section, using the distorted-wave method for relativistic electrons in a Coulomb field. Evaluation of the matrix elements is made in terms of generalized hypergeometric functions, and some numerical results are given for electrons of energy 10 and 100 MeV. Significant enhancement of the virtual radiation spectrum is found to result from the use of distorted waves as opposed to plane waves. Calculations of the contributions of $E1$, $M1$, $E2$, and $E3$ radiation to the bremsstrahlung cross section, $d^2\sigma/d\omega d\Omega$, are also made; enhancement, similar to that observed with the virtual spectrum, is found in this case also.

I. INTRODUCTION

Inelastic scattering of high-energy electrons has been the subject of extensive analysis in the plane-wave Born approximation (for a comprehensive review see Ref. 1). Although this treatment enjoys a most attractive feature, namely, the mathematical simplicity of its results, it is known that plane-wave analysis introduces considerable error when used for scattering from nuclei with large atomic numbers, at least in the calculation of angular distributions.[2] For such nuclei a distorted-wave treatment, using Dirac-Coulomb wave functions for the basis states of the electron, is more effective. Such a calculation can be a laborious task, the chief difficulty being the evaluation of the radial part of the electron matrix element, which requires extensive numerical integration. In some circumstances, particularly for high-angular-momentum components, the electron wave function has no appreciable amplitude in the region near the origin, which is occupied by the nucleus. It is then a reasonable approximation to suppose that the electron is moving in the field of a point charge, which opens up the possibility of expressing the matrix elements in some analytic

form. A closed form for the radial integrals was first obtained for the case where the perturbation is an instantaneous Coulomb interaction.[3] Later results[4] have taken into account retardation explicitly, but in order to achieve a simple form, the electron mass was neglected; this is a common approximation in high-energy electron scattering calculations, and introduces only small errors in the differential cross section. Here, however, we will consider processes for which the amplitude, at least in the plane-wave Born approximation,[5] is logarithmically divergent in the limit $m_e \to 0$. Since the reason for this seems to be the loss of vital kinematical restrictions placed on the system by the finite electron mass, we anticipate that it will be necessary to retain a nonvanishing electron mass in the distorted-wave calculation also. Accordingly, we have developed expressions for the radial integrals with none of the former restrictions[6]; these results are presented in the Appendix.

We use these expressions to consider two calculations which are closely related. The first is the cross section for electron-nucleus excitation integrated over all electron scattering angles; this is the subject of Sec. II. By relating this process to the cross section for the corresponding photoexcitation cross section (σ_γ), a virtual radiation spectrum[7,8] can be synthesized; that is, the total inelastic electron scattering cross section (σ_e) is expressed in a form similar to the yield in photoexcitation experiments:

$$\sigma_e(E) = \int_0^{E-m} \sigma_\gamma(\omega) N(E,\omega)\,\frac{d\omega}{\omega}. \tag{1}$$

In Eq. (1), ω is the energy transfered to the nucleus, E is the incident electron energy, and $N(E,\omega)$ is a spectral function, called the virtual photon spectrum. One can study the photoabsorption cross section experimentally by means of inelastic electron scattering, in the same way as is done with an ordinary source of γ rays (usually bremsstrahlung). Since this involves measuring $\sigma_e(E)$ for a sequence of values of E and unfolding[9] the integral in Eq. (1), a detailed knowledge of the function $N(E,\omega)$ is important. The theoretical evaluation of this spectrum is particularly critical in the case of virtual photons, since, unlike a spectrum of real radiation, it is not directly measurable.

The second process we consider in Sec. III; this is the energy loss by real radiation (bremsstrahlung) for electrons scattering from a nucleus which is not excited in the process. The object is to calculate the cross section, differential in the electron scattering angle and energy loss, which accounts for much of the background in electron scattering experiments. In the distorted-wave method, the cross section develops naturally in the form of a sum of contributions from different orders of multipole radiation. The possibility that such a calculation could be carried out in practice has received comment from Bethe and Maximon,[10] who concluded that it is "virtually impossible." Thus forewarned, we have restricted our numerical results to the contribution of the first electric multipoles, the magnetic terms being found to be negligible in the range considered. Whereas it is certainly necessary to calculate many multipole contributions to attain convergence under all conditions, we do not consider that a full calculation by this method is necessarily impossible.

The use of distorted waves enables one to adopt an especially simple point of view in which the two processes, real and virtual radiation, appear as complementary. Consider the Green function for the propagation of a photon of energy ω, written as a multipole decomposition; the vector part (for which the Green function is a dyadic) is

$$\vec{\vec{G}}(r,r',\omega) = 4\pi i\omega \sum_{\substack{L,M,\\ L'=L,L\pm1}} j_{L'}(\omega r_<) \times h_L^{(1)}(\omega r_>)\vec{Y}_{LL'}^{M*}(\hat{r})\vec{Y}_{LL'}^{M}(\hat{r}'). \tag{2}$$

The photon originates at the electron and propagates either inward, to be detected at the origin by causing a nuclear transition (virtual radiation), or outward, to be detected at infinity (real radiation). The electron coordinate is therefore identified with $r_>$ (the greater of r and r') in the first case and with $r_<$ (the lesser of r and r') in the second case. Since the radial functions are simply related,

$$j_L(\omega r) = \mathrm{Re}\,h_L^{(1)}(\omega r),$$

the electron matrix elements are also related, and the major difference lies in the method of detection. The nucleus will select, at a given energy, only a few (often only one or two) multipole components from the radiation field – those which excite allowed transitions. The virtual radiation spectrum is thus most usefully presented in a form decomposed into separate multipole contributions. The spectrum of real radiation can also be written in this manner, but no practical detector selects such states on the basis of angular momentum; instead the linear momentum of the emitted photon may be detected, or, as we shall assume in this paper, no observation of the photon is made at all. In either case a sum over all multipole contributions must be performed to produce a quantity which corresponds to a physical measurement.

II. VIRTUAL RADIATION

At the conclusion of the previous section we made the assumption that, in virtual radiation, the photon always originates at a point farther from the origin than its point of detection; this denies any significant effect from the electron wave function's penetration of the target nucleus. Such an approximation would be intolerable if the angular distribution of the scattered electrons were to be considered, but the integrated cross section derives almost entirely from the first peak of the angular distribution, and, consequently, is far less sensitive to the finite extent of the nucleus.

Once the no-penetration approximation has been accepted, the nuclear matrix elements entering the problem are just those which arise in the absorption of real radiation. Let $|1\rangle$ and $|2\rangle$ denote the initial and final nuclear states (we consistently use the labels 1 and 2 to distinguish quantities in the initial and final states), and let $\vec{J}_N$ be the nuclear current operator, then write

$$\mathfrak{M}^{(E)}_{L,M}(\omega) = \int d^3r \langle 1|\vec{J}_N(r)|2\rangle \cdot \vec{N}_{L,M}(\omega r) \tag{3}$$

and

$$\mathfrak{M}^{(M)}_{L,M}(\omega) = \int d^3r \langle 1|\vec{J}_N(r)|2\rangle \cdot \vec{M}_{L,M}(\omega r) . \tag{4}$$

In Eqs. (3) and (4) $\vec{N}_{L,M}$ and $\vec{M}_{L,M}$ are the transverse electric and magnetic Hansen solutions,[11] respectively:

$$\vec{N}_{LM}(\omega r) = \left(\frac{L+1}{2L+1}\right)^{1/2} j_{L-1}(\omega r)\vec{Y}^M_{L,L-1}(\hat{r}) - \left(\frac{L}{2L-1}\right)^{1/2} j_{L+1}(\omega r)\vec{Y}^M_{L,L+1}(\hat{r}) , \tag{5}$$

$$\vec{M}_{LM}(\omega r) = j_L(\omega r)\vec{Y}^M_{L,L}(r) . \tag{6}$$

Difficulties arise with the electron matrix elements in proceeding to the limit of no penetration, because the region of integration then includes the origin where the $j = \frac{1}{2}$ angular momentum solutions are mildly divergent (a peculiarity of the solutions of the Dirac equation in a Coulomb field – see Appendix). Divergences in the electron matrix elements can be removed by a technique used in the calculation of internal-conversion coefficients.[12,13] For a given value of L, the radial function $h^{(1)}_L(\omega r)$, appearing in Eq. (1), which diverges most strongly at the origin will have $L' = L+1$. The component $L' = L+1$ can be removed, however, by a gauge transformation. If the vector potential evaluated at the position of the electron r',

$$\vec{A}(r') = \int d^3r\, \vec{G}(r', r)\cdot\vec{J}_N(r) ,$$

is transformed to the least-singular gauge $\vec{\tilde{A}}$ in which

$$\int \vec{\tilde{A}}(r')\cdot\vec{Y}^M_{L,L+1}(\hat{r}')d\Omega_r = 0 ,$$

no divergences occur.[14] The electromagnetic interaction then contains, for a 2^L-pole electric transition, a vector component in which $L' = L-1$, and a scalar part. The interaction Hamiltonian perturbing the electron is then specifically

$$H(\mathrm{EL}) = 4\pi i\omega \sum_M \mathfrak{M}^{(E)}_{L,M}(\omega)\int d^3r \left[\left(\frac{2L+1}{L+1}\right)^{1/2} \times h^{(1)}_{L-1}(\omega r)\vec{j}_e(r)\cdot\vec{Y}^M_{L,L-1}(\hat{r}) + i\left(\frac{L}{2L+1}\right)^{1/2} h^{(1)}_L(\omega r)\rho_e(r)Y^M_L(\hat{r})\right] . \tag{7}$$

For a magnetic transition there is only the vector part with $L' = L$, and this is unchanged by the gauge transformation:

$$H(\mathrm{ML}) = 4\pi i\omega \sum_M \mathfrak{M}^{(M)}_{L,M}(\omega)\int d^3r\, h^{(1)}_L(\omega r)\vec{j}_e(r)\cdot\vec{Y}^M_{L,L}(\hat{r}) . \tag{8}$$

Equations (7) and (8) require the electron charge density ρ_e and current density $\vec{j}_e$ decomposed into spherical harmonics. If we consider a transition between electron angular momentum eigenstates $|\kappa_1\mu_1\rangle$ and $|\kappa_2\mu_2\rangle$, the matrix elements required, when expressed in terms of the wave function given in the Appendix, are

$$\langle\kappa_1\mu_1|\rho_e|\kappa_2\mu_2\rangle = \psi^{\mu_2\dagger}_{\kappa_2}(r)\psi^{\mu_1}_{\kappa_1}(r) ,$$

$$\langle\kappa_1\mu_1|\vec{j}_e|\kappa_2\mu_2\rangle = \psi^{\mu_2\dagger}_{\kappa_2}(r)\vec{\alpha}\psi^{\mu_1}_{\kappa_1}(r) .$$

Using the forms given for ψ^μ_κ in Eq. (A3), and substituting in Eqs. (7) and (8), the angular integration over $d\Omega_r$ can be performed explicitly, rendering $H(\lambda L)$ in the common form

$$H(\lambda L) = 4\pi i\omega \sum_M \mathfrak{M}^{(\lambda)}_{L,M} S(\lambda) I_{L,M}(\kappa_1, \mu_1, \kappa_2, \mu_2) R^{(\lambda)}_L(\kappa_1, \kappa_2) . \tag{9}$$

In Eq. (9), λ is a label which may be E or M for electric or magnetic, $S(\lambda)$ is a projection operator which retains only those terms satisfying the selection rule that $l_1 + l_2 + L$ must be an even integer for electric transitions and an odd integer for magnetic transitions, $I_{L,M}$ is a factor which comes from the angular integral

$$I_{L,M}(\kappa_1, \mu_1, \kappa_2, \mu_2) = (-1)^{j_1+1/2}\left(\frac{2j_1+1}{4\pi}\right)^{1/2} C(j_1, j_2, L; -\tfrac{1}{2}, \tfrac{1}{2}) \times C(j_1, L, j_2; \mu_1, M, \mu_2) , \tag{10}$$

and $R^{(\lambda)}$ is the remaining radial integral over the electron wave functions:

$$R^{(E)}(\kappa_1, L, \kappa_2) = \left(\frac{L}{L+1}\right)^{-1/2} \int_0^\infty r^2 dr \times \Big[h^{(1)}_{L-1}(\omega r)(f_{\kappa_1} g_{\kappa_2} - g_{\kappa_1} f_{\kappa_2}) + \frac{\kappa_1 - \kappa_2}{L} h^{(1)}_{L-1}(\omega r)(f_{\kappa_1} g_{\kappa_2} + g_{\kappa_1} f_{\kappa_2}) - h^{(1)}_{L}(\omega r)(f_{\kappa_1} f_{\kappa_2} + g_{\kappa_1} g_{\kappa_2}) \Big], \quad (11)$$

$$R^{(M)}(\kappa_1, L, \kappa_2) = \frac{\kappa_1 + \kappa_2}{[L(L+1)]^{1/2}} \int_0^\infty r^2 dr \times h^{(1)}_L(\omega r)(f_{\kappa_1} g_{\kappa_2} + g_{\kappa_1} f_{\kappa_2}). \quad (12)$$

By expanding the spherical Hankel function in the finite series

$$h^{(1)}_L(\rho) = -e^{i\rho} \sum_{n=1}^{L+1} \frac{\Gamma(L+n)}{\Gamma(n)\Gamma(L+2-n)} 2^{1-n} i^{n-L} \rho^{-n},$$

and using the explicit expressions for f_κ and g_κ given in the Appendix, the integrals in Eqs. (11) and (12) are reduced to sums of the basic integral

$$I(l,m,n) = \int_0^\infty dr\, r^{\gamma_1+\gamma_2-n} e^{-\Delta r}\, {}_1F_1(\gamma_1 + l - 1 + i\eta_1; 2\gamma_1 + 1; 2ip_1 r)\, {}_1F_1(\gamma_2 + 2 - m - i\eta_2; 2\gamma_2 + 1; -2ip_2 r), \quad (13)$$

where $\Delta = i(p_1 - p_2 - \omega)$. The series solution to the integral of Eq. (13) is given in the Appendix. The expression for the radial integral $R^{(\lambda)}$ in terms of $I(l,m,n)$ is given below:

$$R^{(\lambda)}(\kappa_1, L, \kappa_2) = U_{12} \sum_{n=1}^{L+1} \frac{\Gamma(L+n)}{\Gamma(n)\Gamma(L+2-n)} i^{n-L} (2\omega)^{-n} [A^{(\lambda)}(\xi_1, \xi_2) a_1^* a_2^* I(1,1,n) + A^{(\lambda)}(-\xi_1, -\xi_2) a_1 a_2 I(2,2,n) \pm A^{(\lambda)}(\xi_1, -\xi_2) a_1^* a_2 I(1,2,n) \pm A^{(\lambda)}(-\xi_1, \xi_2) a_1 a_2^* I(2,1,n)]. \quad (14)$$

The upper sign in Eq. (14) is for electric transitions and the lower sign for magnetic transitions. The subsidiary quantities used in the equation are

$$U_{12} = \frac{(2p_1)^{\gamma_1}(2p_2)^{\gamma_2} e^{\pi(\eta_1+\eta_2)/2} |\Gamma(\gamma_1 + i\eta_1)\Gamma(\gamma_2 + i\eta_2)|}{p_1 p_2 \Gamma(2\gamma_1 + 1)\Gamma(2\gamma_2 + 1)},$$

$$a_j = (\gamma + i\eta_j) e^{i\phi_j}, \quad \xi_j = (E_j - m_e)/p_j,$$

$$A^{(E)}(\xi_1, \xi_2) = \left(\frac{L}{L+1}\right)^{1/2} \left\{ 1 - \xi_1\xi_2 + \left[\xi_2 - \xi_1 - \frac{(\kappa_1 - \kappa_2)(\xi_1 + \xi_2)}{L} \right] \frac{L-n+1}{L+n-1} \right\},$$

$$A^{(M)}(\xi_1, \xi_2) = [L(L+1)]^{-1/2} (\kappa_1 + \kappa_2)(\xi_1 + \xi_2).$$

We now have all expressions in Eq. (9) in calculable form, and the final step is to find the cross section.

Suppose that the nucleus undergoes a transition from the ground state to one of a set of final states distinguished by some set of quantum numbers $\{q_i\}$, and the density of such states at excitation energy ω is $\rho_N(\omega, \{q_i\})$. The contribution to the cross section for *photoexcitation* by transitions of multipole character (λL) is

$$\sigma^{(\lambda)}_\gamma(L, \omega) = \frac{8\pi^3}{\omega} \sum_{\{q_i\}} \beta^{(\lambda)}_{(L,\omega)} \rho_N(\omega, \{q_i\}), \quad (15)$$

where $\beta^{(\lambda)}$ is the reduced transition probability defined by

$$\beta^{(\lambda)}(L, \omega) = \frac{2L+1}{2J_1+1} \sum_{M_1} |\mathfrak{M}^{(\lambda)}_{L,M}(\omega)|^2.$$

Since the matrix element for electron-nucleus excitation [Eq. (9)] also contains the factor $\mathfrak{M}^{(\lambda)}_{L,M}$, it is clear that the combination of factors found in Eq. (15) will also occur in the electron cross section for the corresponding process, which thus takes the form

$$\sigma_e(E_1) = \int_0^{E_1 - m_e} \frac{d\omega}{\omega} \left[\sum_{\lambda L} \sigma^{(\lambda)}_\gamma(L, \omega) N^{(\lambda L)}(E, \omega) \right]. \quad (16)$$

A simpler form of Eq. (16), given in Eq. (1), applies when only one multipole order (usually electric dipole) contributes significantly to the cross section. Otherwise it is necessary to take into account the fact that virtual radiation differs from a beam of real radiation, not only in the energy distribution, but also in having a different mixture of multipole orders. Explicit evaluation of the electron cross section is routine, and the details are not given here; the expression found

for $N^{(\lambda L)}$ is

$$N^{(\lambda L)}(E_1,\omega)=\frac{\alpha}{\pi}\frac{p_2}{p_1}\frac{(E_1+m_e)(E_2+m_e)\omega^4}{2L+1}\times\sum_{\kappa_1\kappa_2}S(\lambda)(2j_1+1)(2j_2+1)\times|C(j_1,j_2,L;-\tfrac{1}{2},\tfrac{1}{2})R^{(\lambda)}(\kappa_1,L,\kappa_2)|^2, \quad (17)$$

where it is understood that $E_2=E_1-\omega$, p_i is the electron momentum corresponding to energy E_i, and α is the fine-structure constant.

In numerical calculations it is first necessary to investigate the convergence of the infinite sum over electron partial waves in Eq. (17). When one of the two quantum numbers κ is fixed (say κ_2), the sum over the other is restricted to $(2L+1)$ terms by the selection rules; expression (17) is therefore an unrestricted sum over one variable only. Suppose we restrict the sum to values of $|\kappa_2|\leq n$ and call the partial sum thus obtained N_n, so that Eq. (17) is formally rewritten

$$N^{(\lambda L)}(E_1,\omega)=\lim_{n\to\infty}N_n^{(\lambda L)}(E_1,\omega). \quad (18)$$

An example of the behavior of N_n as n increases is shown in Fig. 1; also shown is the same function when the mass of the electron is set equal to zero. Notice that the contributions from small angular momenta are not significantly changed by the approximation of a massless electron (which may explain why the approximation is acceptable for angular distributions), but that ultimately the series diverges like a harmonic series, unless the finite mass of the electron is included. To find the limit of the sequence (18) we use a standard numerical technique (the epsilon algorithm,[15] incorporated in the IBM scientific subroutine TEAS) so that the error in N is nominally less than 0.1%. Since we are able, at the expense of computer time, to calculate indefinitely many terms in the sequence, this procedure has been verified in a few specific instances.

Since we are primarily interested in the effect on the function $N^{(\lambda L)}$ of including distortion of the electron wave functions, we have concentrated on the calculation of $N(\lambda L)$ as a function of ω for different values of the target charge Z, in comparison with the plane-wave Born approximation.[7] The latter result is actually independent of Z, and should be obtainable from the present formulation by taking the limit of no distortion, $Z\to 0$. We cannot set $Z=0$ precisely, because expression (14) becomes indeterminate; however, for $Z=1$, the result of the present calculation lies within 1.5% of the plane-wave result (which is interesting primarily as a check of our calculation). We then consider the effect of setting $Z=50$, and $Z=92$ (this number is chosen, since the results could be of value in the study of uranium photofission). The results for the three multipole orders $E1$, $M1$, and $E2$ are shown in Figs. (2)–(4); the initial electron energy chosen is $E_1=10$ MeV, and the photon energy ω ranges from 1 to 9 MeV. In every case the effect of the distortion is an enhancement of the spectrum, but the degree of enhancement depends in a complicated manner on the photon energy and multipolarity. In comparing hydrogen as a target with uranium, the $E1$ spectrum is increased 100% for large values of ω but hardly at all for small values. By contrast, the $M1$ spectrum is boosted by a factor 20 over a large range of ω.

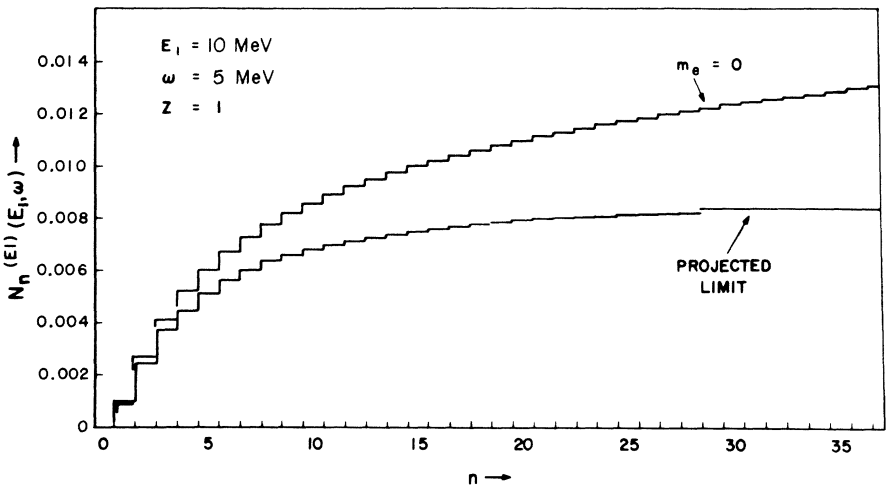

FIG. 1. Convergence of the partial-wave sum N_n [Eq. (18)] for $E1$ virtual radiation with $E_1=10$ MeV, $\omega=5$ MeV, shown as a discrete function of n. Note that convergence is not obtained with a vanishing electron mass (upper staircase); the limit shown for the lower staircase was obtained using the limit projection method TEAS.

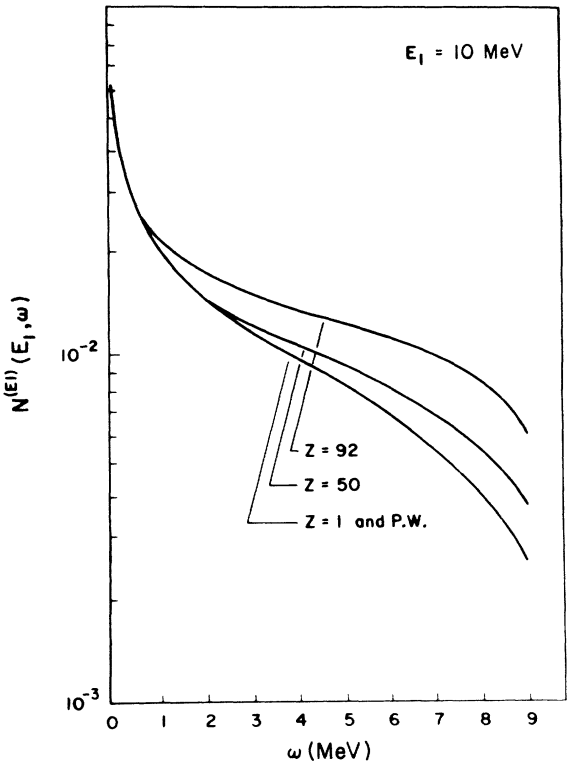

FIG. 2. Virtual photon spectrum for $E1$ radiation from a 10-MeV electron scattering from a nucleus of charge Z. The curves for $Z=1$ and the plane-wave (P.W.) analysis are indistinguishable.

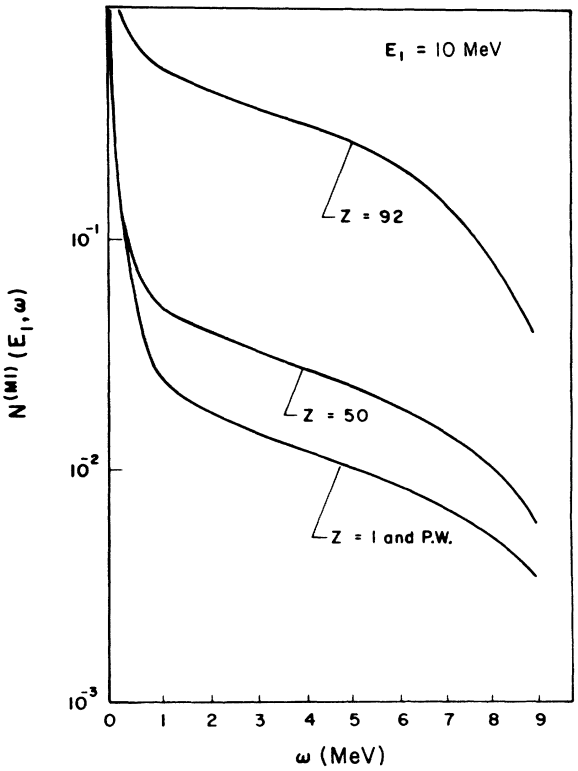

FIG. 3. Virtual photon spectrum for $M1$ radiation. Conditions are the same as for Fig. 2.

We can find no simple way of summarizing these results, and it is not easy to predict the effect of the changed spectrum on the unfolding procedure whereby σ_γ is obtained from the function $\sigma_e(E)$. We feel, however, that we are justified in saying that the distortion cannot be ignored.

III. BREMSSTRAHLUNG CROSS SECTION

In this section we consider the process in which energy loss of the electron is due to bremsstrahlung and not nuclear excitation. The cross section is evaluated as a function of the scattering angle, the initial and final electron energies, and the target charge. It is convenient to treat the field for real radiation in the solenoidal gauge, for which

$$\vec{\nabla}\cdot\vec{A}=0, \quad \text{and } \phi=0,$$

and hence expand the vector potential in terms of the transverse Hansen solutions:

$$\vec{A}(\omega,r)=\sum_{L,M,\omega}\left(\frac{4\pi\omega}{R}\right)^{1/2}[a^\dagger(EL,M,\omega)\vec{N}^*_{L,M}(\omega r) + a^\dagger(ML,M,\omega)\vec{M}^*_{L,M}(\omega r)+\text{H.c.}]. \quad (19)$$

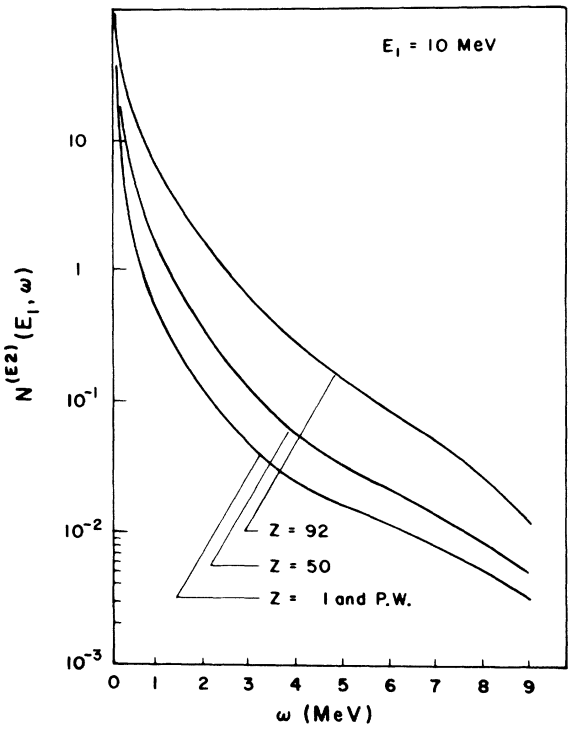

FIG. 4. Virtual photon spectrum for $E2$ radiation. Conditions are the same as for Fig. 2.

In Eq. (19), $a^\dagger(\lambda L, M, \omega)$ is the creation operator for a photon with multipole character λL, projection M, and energy ω; R is the radius of the sphere of normalization. The amplitude for emission of one photon with quantum numbers $\lambda L, M, \omega$ is thus

$$H(\lambda L, M, \omega) = -\int d^3r\, \Psi_2^{(-)\dagger}(\vec{p}_2, r) \times \langle 0 | a(\lambda L, M, \omega) \vec{j}_e \cdot \vec{A} | 0 \rangle \Psi_1^{(+)}(\vec{p}_1, r), \tag{20}$$

where $|0\rangle$ denotes the photon vacuum, and $\Psi_{1,2}^{(\pm)}$ denote the initial and final electron wave functions.

Since the experimental situation envisaged is one in which the angular distribution and energies of the scattered electrons are measured, $\Psi_1^{(+)}$ and $\Psi_2^{(-)}$ are modified plane waves, i.e., solutions of the equation of motion in a Coulomb field which behave asymptotically as ingoing states [denoted by (+)] or outgoing states [denoted by (–)] of definite linear momentum p and spin projection m. When written in terms of the spherical solutions, these are

$$\Psi^{m(\pm)}(\vec{p}, r) = 4\pi \left(\frac{E + m_e}{2EV}\right)^{1/2} \sum_{\kappa\mu} e^{\pm i(\delta_\kappa + l\pi/2)} \times C(l\tfrac{1}{2}j; \mu - m, m) Y_l^{\mu - m}(\hat{p}) \psi_\kappa^\mu(p, r),$$

where V is the normalization volume and the electron quantum numbers E, p, κ, l, j, μ, and m acquire suffixes 1 or 2 to distinguish initial from final quantities. As long as no observation is made of the photons produced, the different radiative multipole orders (λL) contribute incoherently to the cross section, i.e.,

$$\frac{d^2\sigma}{d\Omega\, d\omega} = \sum_{\lambda L} \left(\frac{d^2\sigma}{d\Omega\, d\omega}\right)^{(\lambda L)}, \tag{21}$$

where

$$\left(\frac{d^2\sigma}{d\Omega d\omega}\right)^{(\lambda L)} = \frac{E_1 E_2 p_2 R}{8\pi^3 p_1} V^2 \sum_{m_1, m_2, M} |H(\lambda L, M, \omega)|^2.$$

After explicit evaluation of the vacuum expectation value in Eq. (20) and integration over the angular coordinates, the scattering amplitude may be expressed in terms of radial integrals $\mathcal{R}^{(\lambda)}(\kappa_1, L, \kappa_2)$, which are given explicitly below:

$$\mathcal{R}^{(E)}(\kappa_1, L, \kappa_2) = \frac{1}{[L(L+1)]^{1/2}} \int_0^\infty dr\, r^2 \left\{ \frac{L(L+1) j_L(\omega r)}{\omega r} (f_{\kappa_1} g_{\kappa_2} - g_{\kappa_1} f_{\kappa_2}) + \frac{\kappa_1 - \kappa_2}{\omega r} [\omega r j_{L-1}(\omega r) - L j_L(\omega r)] (f_{\kappa_1} g_{\kappa_2} + g_{\kappa_1} f_{\kappa_2}) \right\},$$

$$\mathcal{R}^{(M)}(\kappa_1, L, \kappa_2) = \frac{\kappa_1 - \kappa_2}{[L(L+1)]^{1/2}} \int_0^\infty dr\, r^2 j_L(\omega r) (f_{\kappa_1} f_{\kappa_2} + g_{\kappa_1} f_{\kappa_2}). \tag{22}$$

The contribution of the general multipole to the cross section is then found to be

$$\left(\frac{d^2\sigma}{d\Omega d\omega}\right)^{(\lambda L)} = [2\alpha(E_1 + m_e)(E_2 + m_e) p_2/p_1] \sum_{m_1 m_2 M} \Big| \sum_{\kappa_1 \kappa_2} S(\lambda) \exp\{i[\delta_{\kappa_1} + \delta_{\kappa_2} + (l_1 - l_2 + 2j_1 + 1)\pi/2]\} Y_{l_2}^{m_1 - M - m_2}(p_2) \times [(2l_1 + 1)(2j_1 + 1)]^{1/2} C(l_1 \tfrac{1}{2} j_1; 0, m_1) C(l_2 \tfrac{1}{2} j_2; m_1 - M - m_2, m_2) \times C(j_1 j_2 L; -\tfrac{1}{2}, \tfrac{1}{2}) C(j_1 L j_2; \tfrac{1}{2}, -M) \mathcal{R}^{(\lambda)}(\kappa_1, L, \kappa_2) \Big|^2. \tag{23}$$

In Eq. (23), $S(\lambda)$ is the projection operator defined in the previous section and δ_κ is the phase shift (see Appendix). To calculate the radial integrals of Eqs. (22), we substitute $h_L^{(1)}(\omega r)$ for $j_L(\omega r)$ and take the real part (all other factors in the integral are real). With this substitution we can again express the radial integrals in terms of $I(l, m, n)$. The magnetic multipole part is particularly simple, for comparison of Eq. (12) for $R^{(M)}$, and Eq. (22) for $\mathcal{R}^{(M)}$, immediately yields

$$\mathcal{R}^{(M)} = \mathrm{Re} R^{(M)}. \tag{24}$$

The electric multipole contribution is somewhat different, but assumes the general form of Eq. (14):

$$\mathcal{R}^{(E)}(\kappa_1, L, \kappa_2) = \mathrm{Re}\left\{ U_{12} \sum_{n=1}^{L+2} \frac{\Gamma(L + n - 1)}{\Gamma(n)\Gamma(L + 3 - n)} i^{n-L} (2\omega)^{-n} [B(\xi_1, \xi_2) a_1^* a_2^* I(1, 1, n) + B(-\xi_1, -\xi_2) a_1 a_2 I(2, 1, n) + B(\xi_1, -\xi_2) a_1^* a_2 I(1, 2, n) + B(-\xi_1, \xi_2) a_1 a_2^* I(2, 1, n)] \right\},$$

where

$$B(\xi_1, \xi_2) = \left(\frac{L}{(L+1)}\right)^{-1/2} \left\{ 2(n-1)(L+1)(\xi_2 - \xi_1) + (\kappa_1 - \kappa_2) \left[(L+1) + \frac{(n-1)(n-2)}{L} \right] (\xi_1 + \xi_2) \right\}. \tag{25}$$

The expression for the cross section, Eq. (23), reduces to a form comparable to Eq. (17) for virtual radiation if the integral over the electron angular distribution is performed; then all sums over magnetic quantum numbers can be carried out explicitly to yield

$$\left(\frac{d\sigma}{d\omega}\right)^{(\lambda L)} = 2\alpha \frac{p_1}{p_2}(E_1+m_e)(E_2+m_e)\sum_{\kappa_1\kappa_2} S(\lambda)(2j_1+1)(2j_2+1)\,|C(j_1 j_2 L;-\tfrac{1}{2},\tfrac{1}{2})\mathcal{R}^{(\lambda)}(\kappa_1, L, \kappa_2)|^2 . \quad (26)$$

We have made no numerical calculation of this expression, since it is unrealistic to determine it experimentally.

For high-energy electrons, a large number of multipole orders will contribute to the sum in Eq. (21). In numerical calculations we examined only the contributions up to $L=3$ in an attempt to decide whether the distorted-wave method could be in serious disagreement with the plane-wave approach of Ref. 5. Since the approximation of plane waves should be best in the limit of high incident energy and a target of low atomic number, we first examine the case $E_1 = 100$ MeV, and $Z=1$. For a fixed energy loss (50%), the predicted angular distribution of scattered electrons is shown in Fig. 5. Since we calculated only a partial sum, and since all terms in the sum (21) are positive, we note that it is consistent that the sum of the first three electric multipoles is less than plane-wave result (magnetic multipole contributions are found to be negligible). Increasing the target charge to $Z=50$, as in Fig. 6, shows that the terms we have calculated increase more rapidly than the Z^2 dependence of the plane-wave Born-approximation result; at backward angles the partial sum actually exceeds plane-wave Born-approximation result. At a lower energy, $E_1 = 10$ MeV, the result for $Z=1$, Fig. 7, is again compatible with the plane-wave result, except in the backward direction. With $Z=50$, the plane-wave Born-approximation result is very obviously too small (Fig. 8). The error in the plane-wave solution has been estimated to be of the same order of magnitude as in large-angle Coulomb scattering,[1] or about $2\alpha \sin\frac{1}{2}\theta$; the present results seem to be in agreement with this but indicate further that the correction is always positive, and is energy dependent.

In the results presented thus far the electron energy loss has been held constant at 50%; we now investigate the cross section as a function of energy loss, holding the scattering angle constant (in this case 60°). The results are shown in Fig. 9 for the case of little distortion ($Z=1$), and Fig. 10 for $Z=50$. Again it is noted that the distorted-wave sum is compatible with the plane-wave result for low Z, but increases more rapidly than Z^2, particularly when the energy loss is small.

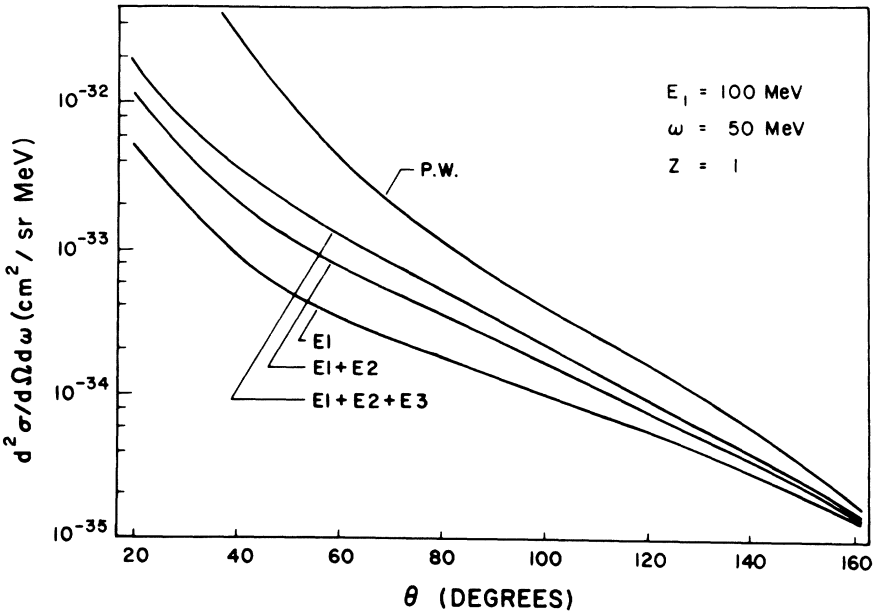

FIG. 5. Angular distribution for radiative scattering of electrons calculated for incident energy 100 MeV, final energy 50 MeV. Energy loss is due to radiation only and not nuclear excitation. Curves labeled $E1$, $E1+E2$, etc., show the effect of adding contributions to different multipole orders of radiation. Since the target charge $Z=1$, the plane-wave (P.W.) result should be a good estimate of the limit obtainable when all orders are included.

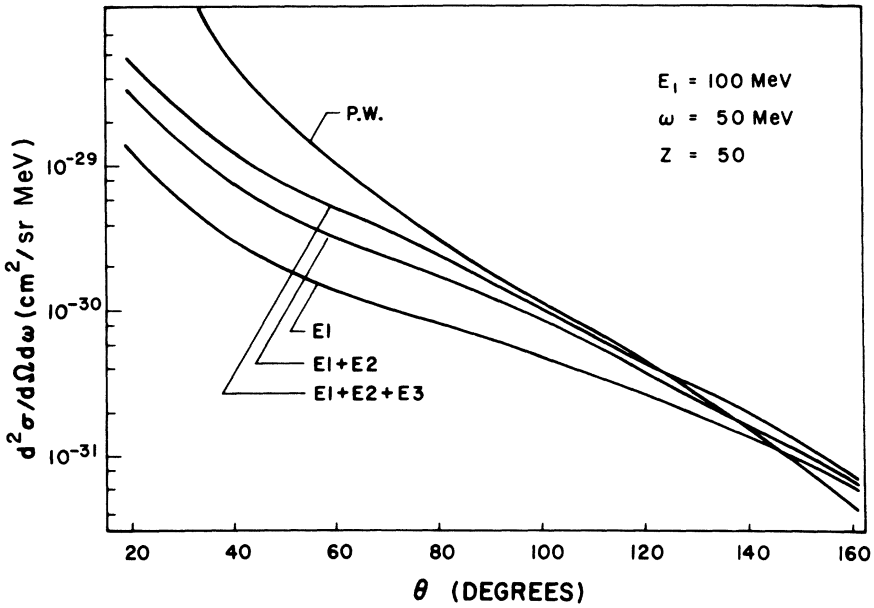

FIG. 6. Angular distribution for electrons calculated for the same condition as Fig. 5, but with $Z = 50$.

In view of the remarks of Sec. I, it would be interesting to establish the behavior of this cross section in the limit of vanishing electron mass. The contribution of each multipole order [Eq. (23)] does not diverge if this approximation is made; in fact, it results in only a small correction in the cases discussed here. If the amplitude is indeed divergent in this limit, we can only suppose that the sum over all orders [Eq. (21)] would not be convergent, but we are unable to establish this.

We have considered the possibility of including transitions of arbitrarily high multipole order. For a given pair of values of κ_1 and κ_2, there is, of course, only a finite number of values of L possible. Moreover, the integrals of the type $I(l, m, n)$, needed to calculate all of these contri-

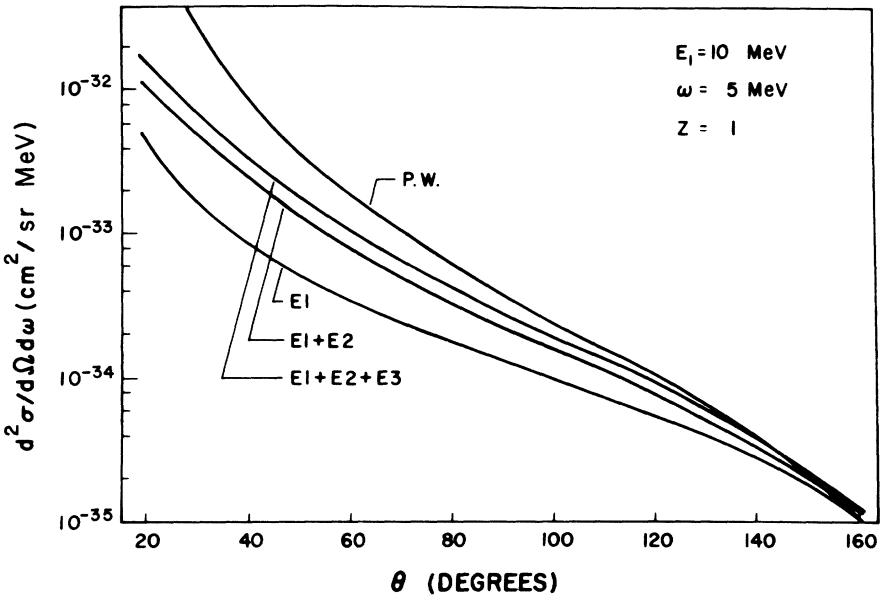

FIG. 7. Angular distribution for radiative scattering of electrons calculated for incident energy 10 MeV, final energy 5 MeV, and target charge $Z = 1$. Approximations in the plane-wave (P.W.) calculation may render it inaccurate at large angles.

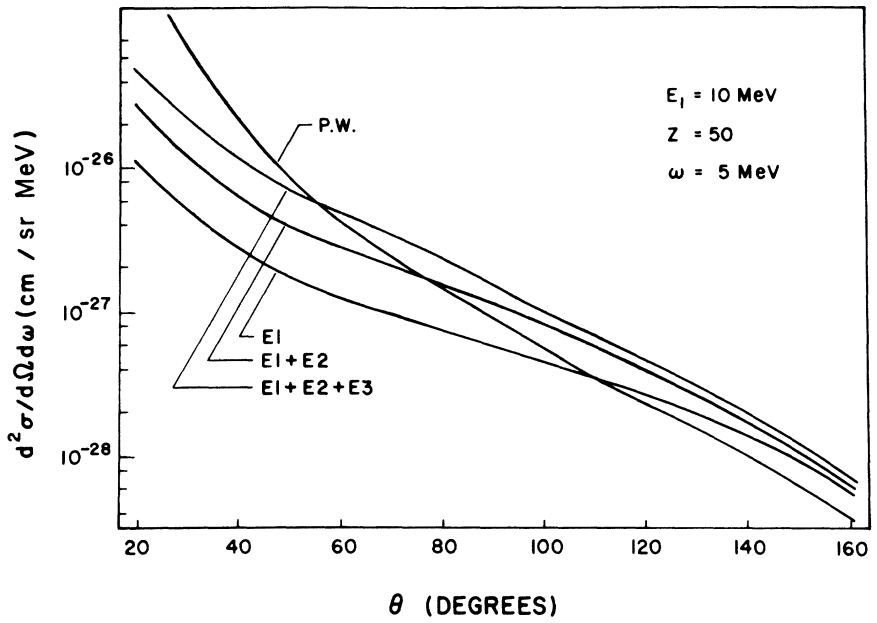

FIG. 8. Angular distribution for electrons calculated for the same conditions as Fig. 7, but with $Z = 50$.

butions, are related by recurrence formulas, with the result that the calculation is not quite as formidable as it might appear.

APPENDIX

The Dirac equation is separable in spherical polar coordinates for any central potential $V(r)$. We write the time-independent equation in the representation[15]

$$[\vec{\alpha}\cdot\vec{p}+\beta m_e+V(r)]\psi=E\psi\,, \tag{A1}$$

where

$$\alpha_i=\begin{pmatrix}0 & \sigma_i\\ \sigma_i & 0\end{pmatrix},\quad \beta=\begin{pmatrix}I_2 & 0\\ 0 & -I_2\end{pmatrix},$$

and σ_i, $i=1,2,3$ are the Pauli spin matrices, I_2 is the 2×2 unit matrix. The angular momentum eigenstates of the electron are conventionally distinguished by the eigenvalues (κ) of the operator

$$K=\begin{pmatrix}\vec{\sigma}\cdot\vec{L}-1 & 0\\ 0 & \vec{\sigma}\cdot\vec{L}+1\end{pmatrix}, \tag{A2}$$

which commutes with the Hamiltonian. Two sub-

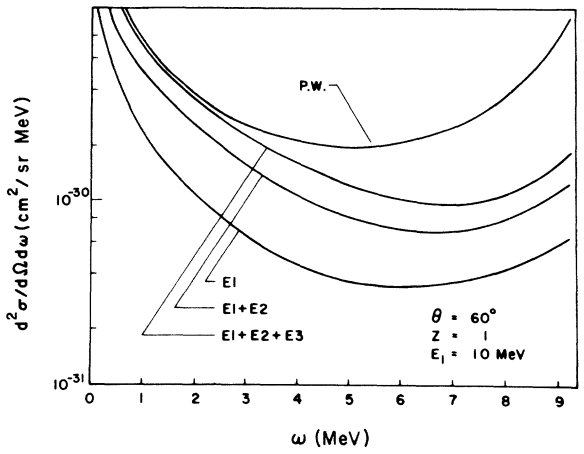

FIG. 9. Radiative energy loss calculated for electrons scattered through a fixed angle ($\theta=60°$). The incident energy is 10 MeV and the distortion ($Z=1$) should be negligible.

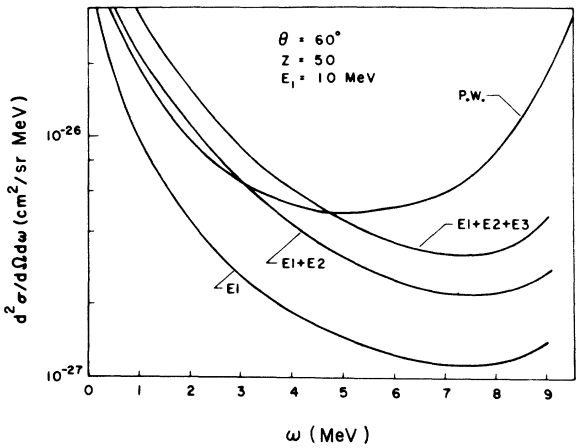

FIG. 10. Radiative energy loss calculated as in Fig. 9 but with $Z=50$.

sidiary quantities j and l are used:

$$j(\kappa) = |\kappa| - \tfrac{1}{2}$$

and

$$l(\kappa) = \kappa \qquad \text{for } \kappa > 0,$$

$$l(\kappa) = \kappa - 1 \quad \text{for } \kappa < 0.$$

In the text the dependence of j and l on κ is generally not shown explicitly, and must be understood. The solutions of Eq. (A1), which are simultaneously eigenfunctions of K, have the form

$$\psi_\kappa^\mu = \begin{pmatrix} g_\kappa(r)\,\chi_\kappa^\mu \\ i f_\kappa(r)\,\chi_{-\kappa}^\mu \end{pmatrix},$$

where the spin-angle functions are

$$\chi_\kappa^\mu = \sum_\tau C(l\tfrac{1}{2}j;\ \mu-\tau,\ \tau) Y_l^{\mu-\tau}(\hat{r})\chi_{1/2}^\tau .$$

For the Coulomb potential, $V(r) = -\alpha Z/r$, the (real) radial functions f_κ and g_κ are given by[16]

$$\begin{pmatrix} f_\kappa \\ g_\kappa \end{pmatrix} = \begin{pmatrix} -(E-m_e)/p \\ 1 \end{pmatrix} \frac{(pr)^{\gamma-1} 2^\gamma e^{\pi\eta/2} |\Gamma(\gamma+i\eta)|}{\Gamma(2\gamma+1)}$$

$$\times \begin{pmatrix} \mathrm{Im} \\ \mathrm{Re} \end{pmatrix} [(\gamma+i\eta) e^{-i(pr-\phi)} \times {}_1F_1(\gamma+1+i\eta;\ 2\gamma+1;\ 2ipr)], \tag{A3}$$

where

$$p = (E^2 - m_e^2)^{1/2},$$

$$\gamma = [\kappa^2 - (\alpha Z)^2]^{1/2},$$

$$\eta = \alpha Z E/p,$$

$$e^{2i\phi} = e^{-i\pi} \frac{\kappa - i\alpha Z m_e/p}{\gamma + i\eta}, \qquad -\pi < \phi < 0.$$

The phase shift of this solution is

$$\delta_\kappa = -\mathrm{Arg}[\Gamma(\gamma+i\eta) + \phi - \gamma\pi/2 + |\kappa|\pi/2]. \tag{A4}$$

For $|\kappa| = 1$, the functions defined in Eq. (A3) are not strictly regular at the origin, because the leading power of r is negative $[\gamma - 1 \simeq -\frac{1}{2}(\alpha Z)^2]$. This divergence is the cause of the problem (see Sec. II) encountered in the limit of a point nucleus.

The electron charge and current densities defined by

$$\rho(r) = \psi_{\kappa_2}^{\mu_2\dagger} \psi_{\kappa_1}^{\mu_1},$$

$$\vec{j}(r) = \psi_{\kappa_2}^{\mu_2\dagger} \vec{\alpha} \psi_{\kappa_1}^{\mu_1},$$

may be resolved into multipole components as follows. Let

$$\int \rho(r) Y_L^M(\hat{r}) d\Omega_r = I_{L,M}(\kappa_1, \mu_1, \kappa_2, \mu_2) \rho_L(r),$$

$$\int \vec{j}(r) \cdot \vec{Y}_{L,L'}^M(\hat{r}) d\Omega_r = I_{L,M}(\kappa_1, \mu, \kappa_2, \mu_2) j_{L,L'}(r),$$

where

$$I_{L,M} = \int \chi_{\kappa_2}^{\mu_2\dagger} Y_L^M \chi_{\kappa_1}^{\mu_1} d\Omega$$

$$= (-1)^{j_1 + \frac{1}{2}} \left(\frac{2j_1+1}{4\pi}\right)^{1/2} C(j_1 j_2 L; -\tfrac{1}{2}, \tfrac{1}{2}) \times C(j_1 L j_2;\ \mu_1, M,\ \mu_2).$$

Then

$$\rho_L = f_{\kappa_1} f_{\kappa_2} + g_{\kappa_1} g_{\kappa_2},$$

$$j_{L,L} = -i \frac{\kappa_1 + \kappa_2}{[L(L+1)]^{1/2}} (f_{\kappa_1} g_{\kappa_2} + g_{\kappa_1} f_{\kappa_2}),$$

$$j_{L,L-1} = -i[L(2L+1)]^{-1/2}[L(f_{\kappa_1} g_{\kappa_2} - g_{\kappa_1} f_{\kappa_2}) + (\kappa_1 - \kappa_2)(f_{\kappa_1} g_{\kappa_2} + g_{\kappa_1} f_{\kappa_2})],$$

$$j_{L,L+1} = i[(2L+1)(L+1)]^{-1/2}[(L+1)(f_{\kappa_1} g_{\kappa_2} - g_{\kappa_1} f_{\kappa_2}) + (\kappa_1 - \kappa_2)(f_{\kappa_1} g_{\kappa_2} + g_{\kappa_1} f_{\kappa_2})].$$

Using the expansion of the spherical Hankel function, as noted in the text, and the expressions (A3) for the radial functions, the multipole matrix elements readily reduce to sums of integrals of the type

$$I(l,m,n) = \int_0^\infty dr\, r^{\gamma_1+\gamma_2-n} e^{i(\omega+p_2-p_1)} {}_1F_1(\gamma_1 + l - 1 + i\eta_1;\ 2\gamma_1+1;\ 2ip_1 r)\, {}_1F_1(\gamma_2 + 2 - m - i\eta_2;\ 2\gamma_2+1;\ -2ip_2 r). \tag{A5}$$

An integral of this form is formally related to one of Appell's double hypergeometric series[17];

$$\int_0^\infty dr\, r^{\alpha-1} e^{-\Delta r} {}_1F_1(a_1;\ b_1;\ k_1 r)\, {}_1F_1(a_2;\ b_2;\ k_2 r) = \Gamma(\alpha)\Delta^{-\alpha} F_2\left(\alpha, a_1, a_2, b_1, b_2, \frac{k_1}{\Delta}, \frac{k_2}{\Delta}\right). \tag{A6}$$

Unfortunately, the series representation for this function does not converge for the values of the variables needed in (A5), namely, $|\Delta| \ll |k_2| < |k_1|$. By using the techniques of analytic continuation, however, we find that it is possible to express the integral in terms of three double hypergeometric series which do converge:

$$F_2(\alpha, a_1, a_2, b_1, b_2, x, y)$$
$$= \Gamma\begin{pmatrix} b_2, a_2-\alpha \\ a_2, b_2-\alpha \end{pmatrix}(-y)^{-\alpha} Q_1\left(\alpha, 1-b_2+\alpha, a_1, 1-a_2+\alpha, b, \frac{1}{y}, \frac{-x}{y}\right)$$
$$+ \Gamma\begin{pmatrix} b_1, b_2, \alpha-a_2, a_1+a_2-\alpha \\ a_1, \alpha, b_2-a_2, b_1+a_2-\alpha \end{pmatrix} Q_2\left(a_2, 1-b_2+a_2, a_1+a_2-\alpha, 1-\alpha+a_2, b_1+a_2-\alpha, \frac{-x}{y}, \frac{1}{\lambda}\right)$$
$$+ \Gamma\begin{pmatrix} b_1, b_2, \alpha-a_1-a_2 \\ \alpha, b_2-a_2, b_1-a_1 \end{pmatrix}(-x)^{-a_1}(-y)^{-a_2} F_3\left(a_1, a_2, 1-b_1+a_1, 1-b_2+a_2, 1+a_2+a_1-\alpha, \frac{1}{x}, \frac{1}{y}\right). \quad \text{(A7)}$$

All series in Eq. (A7) are convergent when $||x|-|y||>1$.[18] The function F_3 is one of the double series of order two investigated by Appell:

$$F_3(a, b, c, d, e, x, y) = \sum_{l,m=0}^{\infty} \frac{(a)_l (b)_m (c)_l (d)_m}{(e)_{l+m} l!\, m!} x^l y^m.$$

The remaining functions Q_1 and Q_2 are double hypergeometric series of order three, with no pedigree that we know of:

$$Q_1(a, b, c, d, e, x, y) = \sum_{l,m=0}^{\infty} \frac{(a)_{l+m} (b)_{l+m} (c)_l}{(d)_{l+m} (e)_l\, l!\, m!} x^l y^m,$$

$$Q_2(a, b, c, d, e, x, y) = \sum_{l,m=0}^{\infty} \frac{(a)_l (b)_l (c)_{l-m}}{(d)_{l-m} (e)_{l-m}\, l!\, m!} x^l y^m.$$

---

*Work supported by the U.S. Army Research Office (Durham).

†Present address: Martin Marietta Corporation, Orlando, Florida.

[1]T. deForest and J. D. Walecka, Advan. Phys. 15, 1 (1966).

[2]T. A. Griffy, D. S. Onley, J. T. Reynolds, and L. C. Biedenharn, Phys. Rev. 128, 833 (1962); D. S. Onley, T. A. Griffy, and J. T. Reynolds, *ibid.* 129, 1689 (1963); D. S. Onley, J. T. Reynolds, and L. E. Wright, *ibid.* 134, 8945 (1964); T. Schucan, Nucl. Phys. 61, 417 (1965).

[3]J. T. Reynolds, D. S. Onley, and L. C. Biedenharn, J. Math. Phys. 5, 411 (1964).

[4]W. W. Gargaro and D. S. Onley, J. Math. Phys. 11, 1191 (1970).

[5]L. C. Maximon and D. B. Isabelle, Phys. Rev. 133, B1344 (1964).

[6]Very similar expressions have been obtained by Olsen and Overbø, private communication; see also, J. D. Rozics and W. R. Johnson, Phys. Rev. 135, B56 (1964).

[7]R. H. Dalitz and D. R. Yennie, Phys. Rev. 105, 1598 (1957).

[8]G. R. Bishop, in *Nuclear Structure and Electromagnetic Interactions,* edited by N. MacDonald (Plenum Press, Inc., New-York, 1965).

[9]A. S. Penfold and J. E. Liess, *Analysis of Photo Cross Sections* (University of Illinios Press, Urbana, Ill., 1958).

[10]H. A. Bethe and L. C. Maximon, Phys. Rev. 93, 768 (1954).

[11]W. W. Hansen, Phys. Rev. 47, 139 (1935).

[12]M. E. Rose, *Multipole Fields* (John Wiley & Sons, Inc., New York, 1955).

[13]L. C. Biedenharn and P. J. Brussaard, *Coulomb Excitation* (Clarendon Press, Oxford, England, 1965).

[14]This is strange, since the theory is gauge invariant, and the point is discussed further in Refs. 12 and 13; we wish to add the following comment. There is no difficulty with a nucleus of finite radius ρ, and the approximation of no penetration is to take the limit $\rho \to 0$. A radial integral R calculated for a finite nucleus can be regarded as a function of ρ which has several representations (different gauges), any one of which can be employed for $\rho > 0$ and the limit of R established as $\rho \to 0$. It does not follow that all representations will converge when evaluated at $\rho = 0$, and it is necessary that we choose one which does include $\rho = 0$ in its realm of convergence – that representation is the least singular gauge.

[15]D. Shanks, J. Math. Phys. 34, 1 (1955); P. Wynn, Nord. Tidskr. Inform. Behandling 3, 175 (1963).

[16]M. E. Rose, *Relativistic Electron Theory* (John Wiley & Sons, Inc., New York, 1961).

[17]P. Appell and J. Kampê de Fêrier, *Fonctions Hypergêométriques et Hypêrspheriques* (Gauthier-Villars, Paris, France, 1926).

[18]A. Erdêlyi, W. Magnus, F. Oberhettinger, and F. G. Tricemi, *Higher Transcendental Functions* (McGraw-Hill Book Company, Inc., New York, 1953), Vol. 1.